Simultaneous Reduction of Arsenic(V) and Uranium(VI) by Mackinawite: Role of Uranyl Arsenate Precipitate Formation

Lyndsay D. Troyer,[†,⊥] Yuanzhi Tang,[‡] and Thomas Borch*[,†,§]

[†]Department of Chemistry, Colorado State University, 1872 Campus Delivery, Fort Collins, Colorado 80523, United States
[‡]School of Earth and Atmospheric Sciences, Georgia Institute of Technology, 311 Ferst Drive, Atlanta, Georgia 30332, United States
[§]Department of Soil and Crop Sciences, Colorado State University, 1170 Campus Delivery, Fort Collins, Colorado 80523, United States

S Supporting Information

ABSTRACT: Uranium (U) and arsenic (As) often occur together naturally and, as a result, can be co-contaminants at sites of uranium mining and processing, yet few studies have examined the simultaneous redox dynamics of U and As. This study examines the influence of arsenate (As(V)) on the reduction of uranyl (U(VI)) by the redox-active mineral mackinawite (FeS). As(V) was added to systems containing 47 or 470 μM U(VI) at concentrations ranging from 0 to 640 μM. In the absence of As(V), U was completely removed from solution and fully reduced to nano-uraninite (nano-UO$_2$). While the addition of As(V) did not reduce U uptake, at As(V) concentrations above 320 μM, the reduction of U(VI) was limited due to the formation of a trögerite-like uranyl arsenate precipitate. The presence of U also significantly inhibited As(V) reduction. While less U(VI) reduction to nano-UO$_2$ may take place in systems with high As(V) concentrations, formation of trögerite-like mineral phases may be an acceptable reclamation end point due to their high stability under oxic conditions.
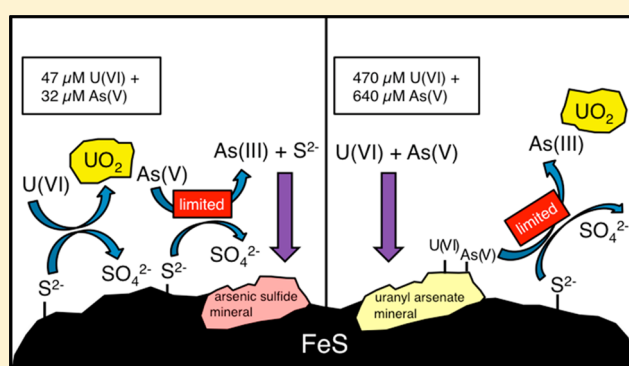
INTRODUCTION

Uranium ore can contain 1.2−10 wt % As, resulting in U and As being found together in sediments at uranium mining or milling sites.[1,2] However, few studies have examined the redox behavior of both U and As under controlled laboratory settings. Under reducing conditions, the most common form of U(IV) is uraninite (UO$_2$), which is sparingly soluble and, therefore, less mobile than aqueous U(VI).[1] The mobility of As under reducing conditions is opposite that of U, with its reduced neutral form under common environmental conditions, As(III) or H$_3$AsO$_3^0$, being more mobile because it is less likely to adsorb onto mineral surfaces at circumneutral pH as compared to its oxidized and charged form, As(V) or H$_2$AsO$_4^-$.[3−6] The difference in mobility of these two toxic elements under similar redox conditions makes remediation of U- and As-containing mine waters and sediments and treatment of waste generated during U ore processing or from in situ recovery (ISR) U mining challenging.[7−9]

When present together, U(VI) and As(V) can form uranyl arsenate aqueous complexes, ternary surface complexes on mineral surfaces, or mineral precipitates such as trögerite (UO$_2$HAsO$_4$·4H$_2$O), depending on their concentrations.[10−13] Although uranyl arsenate aqueous complexes and surface precipitates can form under laboratory conditions, their occurrence in natural systems has not been recorded. Aqueous uranyl arsenate complexes are likely to form under low pH

conditions consistent with acid mine drainage sites, but not under conditions typical of most historic U mining or mill tailings sites.[11] Phosphate can also serve as an analogue for arsenate, as phosphate has similar behavior with uranyl, precipitating as uranyl phosphate minerals at high concentrations and forming ternary complexes on surfaces at low concentrations.[14−16] The formation of low solubility uranyl phosphate minerals has been studied in both laboratory and field-scale experiments as a method of U immobilization alternative to U(VI) reduction to UO$_2$.[14,17−22] Such an alternative remediation strategy is needed at oxic sites where reoxidation of UO$_2$ and remobilization of U is likely to occur. Studies have shown that the presence of aqueous phosphate can also impact the reaction products of U bioreduction,[17,23−27] often leading to the formation of ningyoite-like phases [CaU^{IV}(PO$_4$)$_2$·H$_2$O]. Although studies have examined the effect of As(V) pretreatment on U(VI) sorption to aluminum oxide,[12,28,29] no studies have examined the reactivity of U(VI) in the presence of both As(V) and redox active minerals such as Fe(II) sulfide.

Microbially mediated reduction of U(VI) to uraninite (UO_2) is often used as a remediation strategy for U immobilization.[30,31] During biostimulation, U(VI) can be reduced to UO_2 via direct enzymatic pathways[32−34] or Fe(II)-mediated abiotic pathways such as by mackinawite (FeS). Poorly crystalline mackinawite precipitates when metal- and sulfate-reducing microorganisms use Fe(III) and sulfate, respectively, as electron acceptors either in succession or simultaneously.[35−37] Poorly crystalline mackinawite ages over the course of a few days to crystalline mackinawite.[38−41] In laboratory studies, both synthetic and biogenic mackinawite can reduce U(VI) to nano-UO_2.[42−45] When formed in sediment systems during biostimulation, biomass-associated mackinawite has been shown to be the electron donor responsible for U(VI) reduction to nano-UO_2 and molecular U(IV).[45] Mackinawite can also act as a buffer, protecting UO_2 from reoxidation in biostimulated systems.[43,46,47] In addition to reducing U(VI), mackinawite is also capable of As reduction. As(III) was shown to be reduced to an As–S mineral in the presence of mackinawite.[48,49] As(V) reduction to As(III) has also been shown to occur upon the formation of mackinawite in biostimulated sediment columns, however, As–S mineral formation was not observed due to low aqueous sulfide concentrations.[50,51]

Because of the common presence of As in U ore, the effect of As on U reduction by mackinawite must be considered for the design of U remediation strategies at mine-impacted sites and for the treatment of waste generated by ore processing and in situ recovery mining. While studies have examined the reduction of U and As by mackinawite separately, the two elements have not been investigated together. As(V) pretreatment of aluminum oxide has been shown to increase the uptake of U(VI) due to precipitation of uranyl arsenates on the mineral surface, but little is known about the effect of As(V) on U(VI) reduction or uptake on a redox-active mineral such as mackinawite.[12] No previous studies have investigated the reduction of uranyl arsenate minerals such as trögerite. Thus, in this study, we examine the impact of As(V) on abiotic U(VI) reduction in the presence of mackinawite using complementary laboratory and spectroscopy analysis.

■ EXPERIMENTAL METHODS

Mackinawite Synthesis. Mackinawite synthesis was carried out in an anoxic chamber containing 5% hydrogen and 95% nitrogen. All solutions used were purged with 99.99% pure nitrogen before use. Mackinawite was synthesized by mixing 100 mL of 0.57 M Fe(II) and 75 mL of 1.1 M $Na_2S \cdot 9H_2O$.[43,52] The Fe(II) stock solution was prepared by adding 3.63 g of Fe(0) to 1 M HCl according to Amstaetter et al.[53] in order to ensure that no Fe(III) was present. The mackinawite was allowed to age for 3 days with constant stirring. After aging, the mackinawite was washed by alternating six times between centrifuging at 22095g for 15 min and rinsing with DI water under anoxic conditions. After washing, the mackinawite was freeze-dried overnight under vacuum, ground, and stored anoxically until use.

Batch Experiments. A 5.0 g/L mackinawite suspension was prepared by adding the freeze-dried mackinawite to deoxygenated 0.1 M NaCl in an anoxic chamber. The suspension was allowed to equilibrate for 2 days while stirring. The suspensions were pH adjusted to 7.0 using 1.0 M HCl and allowed to stir for 24 h until the pH had stabilized. The final mackinawite suspension concentration was determined to be

4.7 g/L by dissolving an aliquot of the suspension in 6 M HCl and analyzing for Fe(II) concentration using the Ferrozine method.[54] Stock solutions of 58 mM sodium arsenate and 38 mM uranyl acetate were prepared in DI water and then purged with N_2 before being introduced to the anoxic chamber. Batch experiments were conducted to investigate U(VI) removal from solution at two concentration levels, 47 and 470 μM, hereafter referred to as low U and high U concentration experiments. Sample conditions and sample labels used throughout this manuscript are summarized in Table S1 (Supporting Information). As(V) and U(VI) stock solutions were added to the mackinawite suspension. In cosorption experiments, As(V) was added to both the low and high U treatments over a range of concentrations: 32−320 μM As(V) for the low U concentration treatments and 32−640 μM As(V) for the high U concentration treatments (Table S1, Supporting Information). Experiments were also conducted with single sorbents at both high and low concentrations, including 47 μM U(VI) (U47), 470 μM U(VI) (U470), 85 μM As(V) (As85), and 850 μM As(V) (As850). Each serum bottle contained a total volume of 10 mL. The final concentration of mackinawite in each serum bottle was 4.6 g/L. In order to encourage the precipitation of uranyl arsenate mineral(s), an experiment was also set up where the stock solutions were combined (i.e., 23000 μM U(VI) and 23000 μM As(V)) prior to the addition of the mackinawite suspension and dilution to 10 mL. Following the addition of the mackinawite slurry, the final concentration would have been 350 μM U(VI) and 350 μM As(V), not accounting for possible precipitation. All samples were prepared in triplicate. Samples were reacted for 48 h on a table shaker. After initial setup of the experiments and 48 h of reaction, 1 mL of the suspension was removed with a syringe and filtered through a 0.2 μm nylon filter. Total digestions were performed by combining 1 mL of sample with 1 mL of concentrated HNO_3. One milliliter was sampled following this 48 h reaction period and syringe filtered as described above. Aqueous concentrations of U and As in filtered samples and total digests were determined by using an inductively coupled-plasma mass spectrometer (ICP-MS; Perkin-Elmer Elan DRC-e). The detection limits were 1 ppt for U and 30 ppt for As. Sulfate concentrations in filtered samples were measured using an ion chromatograph (Dionex ICS-2100). Aqueous Fe(II) concentrations were measured using the Ferrozine method.[54] pH was measured in all sample bottles at the beginning and the end of the experiment.

X-ray Absorption Spectroscopy (XAS). Uranium and arsenic X-ray absorption spectroscopy (XAS) was performed at beamline 13-BM-D (GSE-CARS) at the Advanced Photon Source (APS) in Argonne, IL. Fe K-edge EXAFS spectra were collected on the freeze-dried unreacted and reacted solid phase (sample cosorp-U47-As32). Fe XAS was performed at beamline 4-1 (20-pole wiggler) at the Stanford Synchrotron Radiation Lightsource (SSRL) in Menlo Park, CA. From each triplicate, 5 mL of suspension was combined and vacuum filtered onto a 13 mm (diameter) 0.2 μm cellulose acetate membrane filter in an anoxic chamber containing 5% H_2 and 95% N_2. Membranes were enclosed in Kapton polyimide tape, stored, and transported in an anoxic jar (Remel, AnaeroPack Rectangular Jar). Samples were kept in a N_2 environment during U and As XAS data collection. The ring at APS runs at 7 GeV with a current of 100 mA. Energies were selected with a pair of Si (111) monochromators, and spectra were collected in fluorescence mode using a 12-channel Ge detector. The ring

at SSRL runs at 3 GeV with a current of 450 mA. Energies were selected with a pair of Si (220) monochromators, and spectra were collected in fluorescence mode using a wide-angle collection ionization chamber (Lytle detector). For U, extended X-ray absorption fine structure (EXAFS) spectra were collected from −150 to +450 eV around the L_{III}-edge of U (17176 eV). For As, XANES spectra were collected from −150 to +450 eV around the K-edge of As (11876 eV). For Fe, EXAFS spectra were collected from −200 to +1000 eV around the K-edge of Fe (7111 eV). Between two and five spectra were averaged for each sample. During As XANES collection, no beam induced redox damage was observed by comparing the edge position on consecutive scans of the same sample.

Linear combination fitting (LCF) was conducted on the U L_{III}-edge and As K-edge X-ray absorption near edge structure (XANES) data to determine the speciation of U and As and on the Fe K-edge EXAFS data to determine Fe mineralogy. The reference compounds used are (1) for U: trögerite ($U^{VI}O_2HAsO_4·4H_2O$), U(VI) adsorbed to ferrihydrite, and nano-$U^{IV}O_2$; (2) for As: As(V) adsorbed to goethite, As(III) adsorbed to goethite, trögerite ($U^{VI}O_2HAsO_4·4H_2O$), and orpiment (As_2S_3);[53] and (3) for Fe: fresh mackinawite and a mackinawite sample that had been anoxically aged for 3 weeks. While orpiment was used in the LCF described below, this component is referred to as an As–S mineral phase because it could not be distinguished from other As–S mineral reference spectra including realgar (As_4S_4). LCF was performed with reference spectra using the software SixPACK[55] and Athena[56] interfaces to IFEFFIT.[57] Fits are within about ±5% of the mole percentages of fractions for As and Fe LCF and within about ±10% for U LCF.[58−60]

Detailed structure analysis of the U L_{III}-edge EXAFS data was performed with the programs WinXAS[61] and IFEFFIT.[62] Theoretical backscattering paths were calculated using FEFF7[63] and $UO_2HAsO_4·4H_2O$ and UO_2 as model structures. A global threshold energy value (ΔE_0) was allowed to vary during fitting. The amplitude reduction factor, S_0^2, was determined from fitting of the model compounds and was fixed at $S_0^2 = 1$. For U EXAFS, a four-leg axial multiple-scattering (MS) path was included in all samples. This MS path is composed of U−O−U−O with 180° scattering between the center U atom and the two axial O atoms. Errors for the fit parameters are estimated from fits of the model compounds. Error estimates are ±0.01 Å for the R value of the first oxygen shell and ±0.05 Å for higher distance shells. For coordination number, which is heavily correlated to the Debye−Waller factor, the estimated errors are ±20% for the first oxygen shell and ±50% for shells at higher distance. Estimated errors for the Debye−Waller factors are ±0.001 Å² for the first shell and ±0.005 Å² for higher shells. The goodness of fit is evaluated by the residual value.[61]

Thermodynamic Modeling. PHREEQC[64] with the LLNL database was used to calculate the saturation indices for solid phases under the range of U(VI) and As(V) concentrations examined, including uranyl arsenate precipitates such as trögerite [$UO_2HAsO_4·4H_2O$] and [$(UO_2)_3(AsO_4)_2·nH_2O$]. Due to the limited availability of stability constants of the arsenate mineral phases and mackinawite, calculations were carried out on the uranyl-phosphate system in equilibrium with the FeS phase pyrrhotite. Saturation indices were used to predict the potential formation of solid uranyl phosphate and (oxy)hydroxide phases, such as bassettite [$Fe(UO_2)_2(PO_4)_2·8H_2O$], autunite [$Ca(UO_2)_2(PO_4)_2·nH_2O$], chernikovite

[$UO_2HPO_4·4H_2O$], [$(UO_2)_3(PO_4)_2·nH_2O$], and schoepite [$(UO_2)_8O_2(OH)_{12}·12H_2O$)].

■ RESULTS

Mackinawite Characterization and Aqueous Chemistry. Based on LCF of Fe K-edge EXAFS (Figure S1, Supporting Information), the mackinawite structure prior to reaction was similar to the freshly precipitated mackinawite reference. The reacted mackinawite was fit with 18% of the freshly precipitated mackinawite reference and 82% of the mackinawite reference that was aged anoxically for 3 weeks (Table S2, Supporting Information). Aqueous concentrations of Fe(II) decreased while sulfate concentrations increased over the 48 h reaction period in all treatments (Table S3, Supporting Information).

U and As Removal from Solution. The amount of U and As removed from the aqueous phase is summarized in Figure S2 and Table S4 (Supporting Information). In all treatments, 100% of U was removed from the aqueous phase at the end of the 48 h reaction time. Arsenic removal varied by initial As(V) concentration but was complete at the lowest concentration of As(V) (32 μM; samples cosorp-U47-As32 and cosorp-U470-As32). In the low U concentration experiments, As(V) removal decreased with increasing concentration from 100% in cosorp-U47-As32 to 92% in cosorp-U47-As320. As(V) removal also decreased in the high U concentration experiments from 100% in cosorp-U470-As32 to 93% in cosorp-U470-As640. In the absence of U (As85 and As850), As removal was limited. At the low concentration (As85), 28% of As was removed from solution, and at the high concentration (As850) 20% of As was removed. To further examine the removal mechanism(s) for U(VI) and As(V) from solution, XANES and EXAFS spectroscopy were performed on the reacted solid phase.
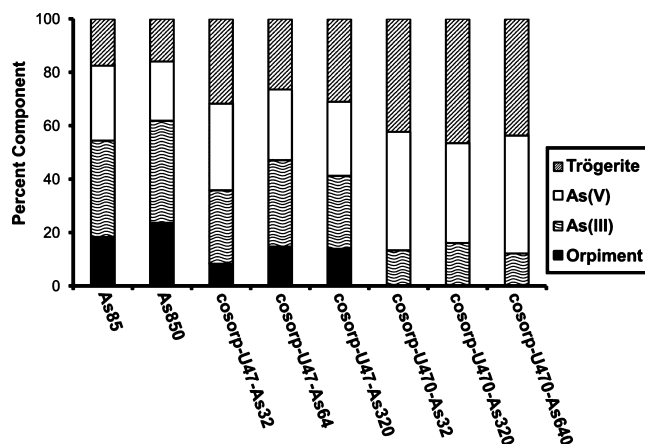
Extent of Reduction of Solid Phase-Associated U(VI) and As(V). *Uranium Speciation.* XANES spectroscopy was used to identify the distribution of U and As species associated with mackinawite. Three U reference compounds (nano-UO_2, U(VI) adsorbed to ferrihydrite, and trögerite) were included in LCF to model the possible mechanism(s) of U(VI) removal from the suspension, namely, reductive precipitation, surface adsorption, and precipitation with As(V), respectively. The results of LCF of U XANES data are summarized in Figure 1, Figure S3, and Table S5 (Supporting Information). In all systems, XANES fits were best represented by the combination of nano-UO_2 and trögerite standards, with the exception of cosorp-U470-As640 which was fit with 15% nano-UO_2, 29% U(VI) adsorbed to ferrihydrite, and 56% trögerite. In the absence of As(V), all solid-phase U is present as nano-UO_2 at both U concentrations. In low U concentration systems, As(V) had limited impact on the extent of U reduction. In cosorp-U47-As32, U(VI) was 100% reduced, similar to the U47 system, indicating that As had no impact on U reduction at this concentration level. As As(V) concentrations increased, U(VI) reduction by mackinawite was inhibited. Nano-UO_2 was 100% of the total solid-phase U in cosorp-U47-As64, but decreased to 90% in cosorp-U47-As320. As(V) had a greater impact on U reduction in high U concentration systems. In cosorp-U470-As32, U reduction was complete, similar to the As(V)-free treatment. In cosorp-U470-As320, 75% of the solid-phase U was in the form of nano-UO_2. The greatest effect on U(VI) reduction was observed in cosorp-U470-As640 where only 15% of the solid phase U was nano-UO_2.

14328

dx.doi.org/10.1021/es5037496 | Environ. Sci. Technol. 2014, 48, 14326−14334
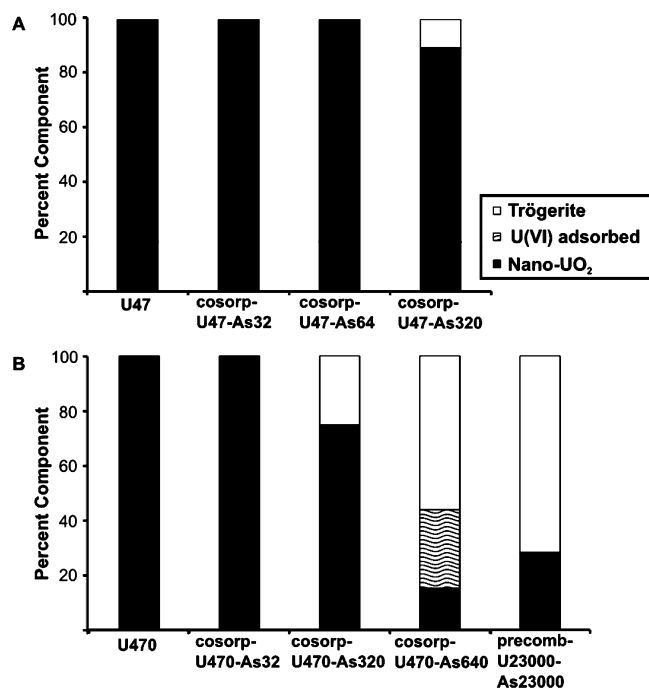
Figure 1. Percent distribution of U in the solid-phase reaction products collected after 48 h of reaction in systems containing (a) 47 μM U(VI) and (b) 470 μM U(VI) with varying concentrations of As(V), 4.6 g/L of mackinawite, and 0.1 M NaCl as determined by linear-combination fitting of U L_{III}-edge XANES. Reference compounds used for linear-combination fitting include trögerite, U(VI) adsorbed to ferrihydrite, and nano-UO$_2$. Solid-phase reaction products of triplicate systems were combined prior to analysis.

Figure 2. Arsenic redox speciation of solid phase reaction products from batch experiments as determined by linear combination fitting of As K-edge XANES spectra. Spectra were fit using four standards including trögerite (UO$_2$HAsO$_4$·4H$_2$O), As(V) adsorbed to goethite, As(III) adsorbed to goethite, and orpiment (As$_2$S$_3$). Batch reactors contained 4.6 g/L mackinawite, 0.1 M NaCl, and 85 μM As(V), or 850 μM As(V) in the absence of U(VI) or with 47 μM U(VI) or 470 μM U(VI) with varying concentrations of As(V) and were reacted for 48 h.

In order to study the role of possible precipitation of uranyl arsenate mineral phase(s) (e.g., trögerite) on the reduction of U(VI), the extent of U(VI) reduction was also examined in an experiment (precomb-U23000-As23000) where U(VI) and As(V) were combined prior to the addition of mackinawite suspension. In this system, only 37% of U(VI) was reduced in comparison to 75% reduction in cosorp-U470-As320, which is the sample which is closest to the As and U concentrations in precomb-U23000-As23000 following dilution with the mackinawite slurry.

Arsenic Speciation. The percentage of reduced As species associated with the solid phase was determined by LCF of As XANES spectra. The results of the fitting are summarized in Table S6 (Supporting Information), Figure 2, and Figure S5 (Supporting Information). In the low U concentration systems, 36−41% of the solid-phase associated As was reduced to As(III) at all added As(V) concentrations. In the high U concentration systems, less As(V) reduction occurred, with 12−16% reduced to As(III) for all of the added As(V) concentrations. Complete reduction was not observed. To rule out the possibility that U(VI) may limit As(V) reduction, As(V) was combined with mackinawite at 85 and 850 μM without U(VI) addition (samples As85 and As850). In As85, 60% of solid-phase As was reduced, whereas in As850, 67% of solid-phase As was reduced, demonstrating that complete reduction of As(V) did not occur even in the absence of U(VI). As(V) reduction was also investigated in precomb-U23000-As23000. Similar to U(VI), the percentage of As(V) reduction was lower in precomb-U23000-As23000 (6%) (350 μM U(VI) and 350 μM As(V) following dilution with mackinawite slurry) than in the comparable sample, cosorp-U470-As320 (16%).

Thermodynamic modeling was performed to help determine the most likely aqueous complexes and mineral phases present at equilibrium for all of the As(V) treatments.

Thermodynamic Modeling. Thermodynamic modeling was performed using the program PHREEQC to determine if the conditions of each experimental treatment favored precipitation of U mineral phases in equilibrium with FeS. Results of the modeling are summarized in Table S7 (Supporting Information). Limited information was available on the thermodynamic constants of uranyl arsenate aqueous complexes and solid phases. Rutsch et al.[10] compared the formation constants of three uranyl arsenate aqueous complexes using time-resolved laser-induced fluorescence spectroscopy (TR-LFS) and found their values to be similar to their uranyl phosphate analogues. Therefore, we conducted the calculations using phosphate as a chemical analogue for arsenate because of their similar stability constants.[10] Modeling was performed primarily to determine if the formation of uranyl arsenate mineral phases was favored. The formation of two possible uranyl phosphate minerals was considered, including chernikovite (UO$_2$HPO$_4$·4H$_2$O) and (UO$_2$)$_3$(PO$_4$)$_2$·nH$_2$O. However, (UO$_2$)$_3$(AsO$_4$)$_2$·12H$_2$O has never been found to occur in nature,[29] so we will only report saturation indices for chernikovite, which is an analogue for the As-containing phase trögerite (UO$_2$HAsO$_4$·4H$_2$O). For all concentrations of As(V) (32−320 μM) in the low U concentration experiments, systems were undersaturated for chernikovite. The high U concentration systems were also undersaturated for chernikovite with 32 μM As(V) (cosorp-U470-As32), but slightly saturated with 320 and 640 μM As(V) (cosorp−U470-As320 and cosorp-U470-As640) with calculated saturation indices of 0.35 and 0.62, respectively. The saturation indices were modeled in the absence of FeS for the precomb-U23000-As23000 treatment. Oversaturation of U phosphate mineral phases include (UO$_2$)$_3$(PO$_4$)$_2$·4H$_2$O and H$_2$(UO$_2$)$_2$(PO$_4$)$_2$ (Table S6, Supporting Information). We also observed a visible yellow precipitate in this treatment. The saturation indices for chernikovite support that trögerite is an appropriate reference compound to be used as the U(VI) standard in the LC fitting of

U XANES data. Thus, EXAFS spectra were collected and interpreted in order to elucidate the potential role of trögerite. Calculations indicate oversaturation for reduced U minerals phases (UO_2) for all systems in the presence of FeS (Table S7, Supporting Information). We also observed oversaturation for uranyl oxyhydroxides in the precomb-U23000-As23000 system, showing that other U(VI) minerals may be present in addition to the U(VI) phosphate mineral phases.

Characterization of Solid Phase-Associated U. The Fourier transform of U L_{III}-edge EXAFS data was fit shell-by-shell for selected samples in order to determine the local structure of U(VI) and U(IV) species in the final reaction products. The fitting parameters are summarized in Table 1.

Table 1. Summary of U L_{III}-edge EXAFS Fitting Results for Selected U(VI) and As(V) Treatments

shell	CN[a]	R (Å)	σ^2 (Å^2)	E_0 (eV)	residual[b] (%)
cosorp-U470-As320					
O	5.7	2.31	0.012	0.6	13.3
U	4.0	3.69	0.017		
cosorp−U470-As640					
O_{ax}	1.6	1.78	0.003	2.55	8.1
O_{eq}	6.4	2.26	0.011		
As	1.8	3.68	0.008		
precomb-U23000-As23000					
O_{ax}	2.4	1.84	0.008	6.78	7.5
O_{eq}	6.3	2.29	0.009		
As	1.2	3.71	0.002		

[a]Coordination number. [b]The residual is calculated as

$$\text{residual (\%)} = \sum_{i=1}^{N} |y_{exp}(i) - y_{theo}(i)| \sum_{i=1}^{N} |y_{exp}(i)| \times 100$$

The three reported samples were chosen due to the difference in experimental setup and the observed distribution of U redox species as determined by LCF of XANES spectra. The three selected treatments were (1) cosorp-U470-As320, (2) cosorp-U470-As640, and (3) precomb-U23000-As23000. The data for each of these samples and their corresponding fits are shown in Figure 3. Of all of the treatments, cosorp-U470-As640 and precomb-U23000-As23000 had the highest percentage of U(VI) in the solid reaction products as determined by LCF of U XANES. The overall fitting results indicated that both of these treatments contained a trögerite-like U(VI) mineral. The first broad peak at ~1.5 Å in R space (without phase correction; Figure 3) is consistent with the combined contribution from the axial and equatorial oxygen atoms. The peak at ~3.4 Å in R space (without phase correction) corresponds to contributions from the U−As path and the U−O_{ax}−U−O_{ax} multiple scattering path. In contrast to these two treatments, cosorp-U470-As320 was dominated by a U(IV) species with a structure similar to nano-UO_2 as indicated by LCF of U XANES data, which is consistent with our shell-by-shell EXAFS fitting results. The peak at ~1.9 Å in R space (without phase correction) is indicative of the backscattering from the first shell oxygen atom. The peak observed at ~3.7 Å in R space at the U−U distance has a U coordination number of ~4. This suggests the dominant presence of nanosized UO_2, as no U−U correlation will be observed for monomeric U(IV) species[23,25] and a greater amplitude of this shell will be observed for highly
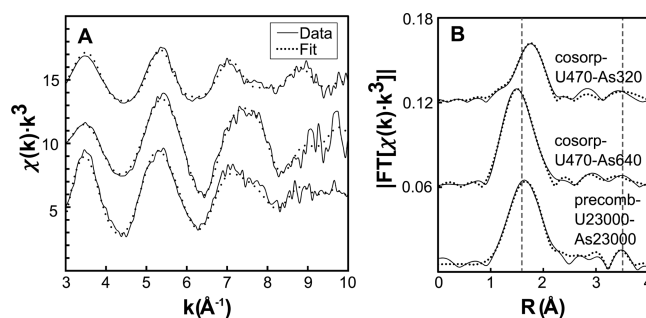
Figure 3. (A) k^3-weighted L_{III}-edge U EXAFS data of selected cosorption and precombination samples including cosorp-U470-As320, cosorp-U470-As640, and precomb-U23000-As23000 and (b) corresponding Fourier Transforms (not corrected for phase shift). Spectra (solid line) and fits (dotted line) are both plotted. Cosorption experiments contained 4.6 g/L mackinawite, 0.1 M NaCl, and either 470 μM U(VI) and 320 μM As(V) or 470 μM U(VI) and 640 μM As(V) added to the mackinawite suspension. In the precombination experiment, 23000 μM U(VI) and 23000 μM As(V) were combined prior to the addition of the mackinawite slurry. All experiments reacted for 48 h.

crystalline or long-ranged ordered UO_2, which has a coordination number of 12 as compared to 4 in our system The U−O and U−U coordination numbers are consistent with nano-UO_2 formed in previous studies with mackinawite and dissolved sulfide.[43,65]

■ DISCUSSION

While limited reduction of U(VI) to U(IV) in the presence of mackinawite was observed in early work,[66] two recent studies have observed complete reduction of U(VI) to U(IV).[43,44] In agreement with these studies, we also observed 100% sorption of U(VI) to mackinawite followed by complete reduction of U(VI) to nano-UO_2 in the absence of As(V) (samples U47 and U470) after 48 h of reaction time (Table S5, Supporting Information). Previous studies observed uptake of U(VI) onto the mackinawite surface within 15 min at pH 7, while reduction of U(VI) followed uptake and occurred on a longer time scale of 4 h.[42] Although we did not conduct a time dependent study, U(VI) was fully reduced in samples without As(V) upon immediate mixing with mackinawite and filtration (Table S5, Supporting Information), suggesting immediate reduction of U(VI) and precipitation as the cause of removal from solution. While complete reduction of U(VI) was not observed with all concentrations of As(V), aqueous U(VI) was completely removed by mackinawite in all treatments.[42−44,66] Based on previous research on the effect of arsenate and phosphate on U(VI) interactions with aluminum oxides and goethite,[12,14,15] we expect the primary form of solid-phase U(VI) to be uranyl arsenate surface precipitate(s), although we cannot rule out the possible presence of adsorbed ternary uranyl arsenate surface complexes.

Two major mechanisms have been suggested for the reduction of U(VI) to UO_2 by mackinawite. Hua et al.[42] proposed that U(VI) could be reduced by either structural Fe(II) or $S^{2−}$ but could not distinguish between the two. Hyun et al.[43] and Veeramani et al.[44] both suggested that U(VI) was reduced by structural $S^{2−}$ rather than Fe(II), but the two studies proposed different oxidation products of $S^{2−}$, namely elemental sulfur and sulfate, respectively. Our results are most consistent with the mechanism proposed by Veeramani et al.[44] because we

observed an increase in aqueous sulfate concentrations in all systems (Table S2, Supporting Information). In other studies, an increase in aqueous Fe(II) concentrations was observed following reaction which indicated the exchange of structural Fe(II) for UO_2^{2+} as U(VI) adsorption takes place.[42,43] We measured a decrease in aqueous Fe(II) concentrations over the reaction period which rules out the possibility of exchange between Fe(II) and U(VI). We did not observe conversion of mackinawite to other mineral phases following the reaction period, suggesting that there was also no oxidation of structural Fe(II). Fe EXAFS data (Figure S1, Supporting Information) show that the mackinawite structure was consistent with nanoparticulate mackinawite at the start of the experiment and was dominated by crystalline mackinawite at the end of the experiment, consistent with previous studies showing the conversion of mackinawite from nanoparticulate to crystalline over the period of days.[67]

In this study, we examine the effect of As(V) on the reduction of U(VI) by mackinawite. Here, we observe that As(V) limits U(VI) reduction at high concentration due to the formation of trögerite-like uranyl arsenate precipitates. Although the effect of As(V) on U(VI) reduction has not been previously studied, phosphate has been shown to affect the product of U(VI) reduction. Phosphate present in biomass is thought to promote the formation of molecular U(IV) rather than crystalline UO_2,[17,23,25] which was not detected in our study. However, due to the limited sensitivity of XAS, we cannot rule out the possible existence of minor amounts of molecular U(IV) in our system, which could be masked by other more dominant U components. Studies have also found that microbially mediated reduction of U(VI) in the presence of aqueous phosphate or as hydrogen uranyl phosphate $(UO_2HPO_4 \cdot 4H_2O)$ results in the formation of the U(IV) phosphate mineral ningyoite $[CaU(PO_4)_2]$.[17,23-27] Few reports have discussed the existence of a similar U(IV) arsenate mineral phase,[68] and LCF of our XANES and EXAFS did not indicate the presence of a U(IV)−As(V) mineral.

The ability for trögerite-like uranyl arsenate precipitates to be reduced by mackinawite was also investigated to elucidate if their formation prevents the reduction of both U(VI) and As(V). In precomb-U23000-As23000, the presence of a uranyl arsenate precipitate with a structure similar to trögerite $(UO_2HAsO_4 \cdot 4H_2O)$ was confirmed by shell-by-shell fitting of the U L_{III}-edge EXAFS spectrum. The peak observed at ∼3.4 Å in R space is the indication of a backscattering contribution from As atoms. $UO_2(HAsO_4)_2 \cdot H_2O$ was not present in our system based on U EXAFS data.[12,29] $UO_2(HAsO_4)_2 \cdot H_2O$ is also not known to occur naturally.[69,70] Less U(VI) reduction (39%) was observed in the precomb-U23000-As23000 sample as compared to the system where U(VI) and As(V) were added directly to the mackinawite suspension (75%) (cosorp-U470-As320). Rui et al.[26] showed that the microbial reduction of U(VI) present as hydrogen uranyl phosphate takes place following mineral dissolution despite the limited solubility of this mineral phase. Despite a longer reaction time, Rui et al.[26] observed only partial reduction of the hydrogen uranyl phosphate. With the presence of low solubility uranyl arsenate precipitates in our system (K_{sp} of $(UO_2)_3(AsO_4)_2 \cdot 12H_2O$ is 4.07×10^{-51}),[13] we expect a decreased degree of U(VI) reduction where uranyl arsenate precipitates occur, which was confirmed in our system. There is also a possibility that the reduced U found in the precomb-U23000-As23000 sample resulted from reduction of U(VI) remaining in solution

following uranyl arsenate precipitation rather than from the reduction of mineralized U(VI).

Our system also examined the redox behavior of As in the presence of mackinawite. While some reduction of As(V) occurred, we did not observe complete reduction in any of the treatments (Figure 2 and Table S6, Supporting Information). Based on the findings of Gallegos et al.,[49] As can be reduced by structural S^{2-} on the mackinawite surface, which is similar to the mechanism for U(VI) reduction. Less removal of As from the aqueous phase was observed in treatments containing U than in those without, indicating that U limited As uptake. With the formation of surface precipitates (UO_2 or uranyl arsenate precipitates), U(VI) may limit As(V) reduction by preventing As(V) interaction with surface S^{2-} groups. The number of reactive surface sites present on mackinawite (6.4×10^{19} sites), as estimated by the surface area and reactive site density measured by Wolthers et al.,[69] are sufficient for all U(VI) and As(V) to be adsorbed by inner-sphere complexation even in the high U concentration systems.[71,72] Even though the number of estimated reactive surface sites on mackinawite was sufficient to adsorb all of the added As(V) in both low and high U concentration treatments, studies have found that As has low affinity for mackinawite.[50,73,74] According to Widler et al.[75] and Bebie et al.,[76] the point of zero charge (PZC) of mackinawite is 2−3, so the surface of mackinawite would be negatively charged in our system (pH 6.7−7.5), likely resulting in preferential adsorption of uranyl cations over arsenate anions.[73] Although the PZC of crystalline mackinawite was measured by acid−base titration to be 7.5 by Wolthers et al.,[71] they attribute the difference in their value from that of Widler et al.[75] to be due to oxidation at the mackinawite surface in the previous measurements. While mackinawite was present in an oxygen-free system in our experiments, the surface may more closely resemble that in Widler et al.[75] than in Wolthers et al.,[71] where the mackinawite surface was continually renewed by dissolution during titration.

Based on XANES fitting, As(III) resulted from As(V) reduction. The extent of reduction was greater in single sorbent systems (As85 and As850) than in the cosorption systems. As previously discussed, As may have less contact with the mackinawite surface when U is also present due to the formation of trögerite-like surface precipitates and preferential U adsorption.[77] The formation of an As−S mineral phase (e.g., realgar, arsenopyrite and orpiment) was indicated in low U concentration systems and systems without U. Past studies have observed that the reduction of As by mackinawite results in As−S mineral precipitation.[48,49] An As−S mineral phase was present in some samples at 8−27% of the total As (Table S6, Supporting Information), but the extent of reduction to an As−S mineral phase was less than was observed by Gallegos et al.[49] The formation of As−S mineral precipitates in our study may be limited to the low U concentration systems and the single sorbent systems because precipitation is favored only under a narrow range of sulfide concentrations. Burton et al.[51] found that As and sulfide concentrations must be greater than the solubility of As−S mineral phases for precipitation to occur but that higher sulfide concentrations favor dissolved thioarsenic species formation. While sulfide concentrations may be too low to favor As−S mineral precipitation, aqueous thioarsenic species may be present as they have been shown to form under low sulfide concentrations in Fe-containing systems.[78−80] Gallegos et al.[49] observed that thioarsenite may be found in systems containing As(III) and mackinawite, but we expect that

thioarsenate species would be favored. Thioarsenites are subject to rapid oxidation in the presence of elemental sulfur which likely forms as an intermediate in sulfide oxidation to sulfate.[81] The presence of thioarsenates may also explain the limited observed adsorption of As because Couture et al.[80] found that monothioarsenate and tetrathioarsenate both adsorb to mackinawite but to a lesser extent than arsenate or arsenite. Our observation of limited As–S mineral formation at all concentrations is consistent with other work where low aqueous sulfide concentrations were observed to prevent As–S mineral formation.[50,51] Because As(III) is the more mobile and more toxic form of As,[82] the presence of U in systems may increase overall As removal from solution as well as preventing reduction to its more mobile form.

Biogenic mackinawite has been shown to play an important role in the reduction of U(VI) in sediments at U mill tailings such as those in Rifle, CO.[45] Previous work and this study have also shown that mackinawite can prevent reoxidation of UO_2 (see the Supporting Information), subsequently preventing U remobilization. While studies have examined the ability of U(VI) to be reduced by synthetic and biogenic mackinawite, the effect of naturally occurring anions on U(VI) reduction has not been investigated.[43,44] An improved understanding on the influence of U-complexing anions (e.g., arsenate, vanadate, and phosphate) on U(VI) reduction will help us to better predict U(VI) reduction and retardation in environmental systems. The high concentrations of As(V) and U(VI) used in this study may not occur naturally at most open-pit mine tailings, but they may occur in drainage from in situ leaching U mining or from the processing of U ore.[11] Because a common strategy for immobilization of U is reduction to UO_2, understanding whether arsenate or similar anions such as phosphate or vanadate can limit reduction is important for the design of remediation strategies.[17,83,84] While the presence of stable U(VI) mineral phases may prevent U(VI) reduction, their formation may offer an alternative strategy for U immobilization. Further research into the influence of anions such as carbonate (see the Supporting Information), phosphate, vanadate, and arsenate is needed to better understand if U(VI) reduction by mackinawite is a significant process in all natural systems.

■ ASSOCIATED CONTENT

Ⓢ Supporting Information

Discussion of reoxidation experiments and experiments including bicarbonate. Additional figures include Fe EXAFS spectra, U and As XANES spectra, As and U removal from the aqueous phase, extent of U reoxidation, additional tables summarizing sample conditions, Fe, As, and U LCF, aqueous Fe and sulfate concentrations, and modeled saturation indices. This material is available free of charge via the Internet at http://pubs.acs.org.

■ AUTHOR INFORMATION

Corresponding Author
*E-mail: thomas.borch@colostate.edu. Tel: +1-970-491-6235.

Present Address
[⊥]Department of Earth and Planetary Sciences, Washington University, St. Louis, Missouri 63130, United States

Notes
The authors declare no competing financial interest.

■ REFERENCES

(1) Abdelouas, A. Uranium mill tailings: geochemistry, mineralogy, and environmental impact. *Elements* **2006**, *2* (6), 335.
(2) Donahue, R.; Hendry, M. J. Geochemistry of arsenic in uranium mine mill tailings, Saskatchewan, Canada. *Appl. Geochem.* **2003**, *18* (11), 1733–1750.
(3) Dixit, S.; Hering, J. G. Comparison of arsenic(V) and arsenic(III) sorption onto iron oxide minerals: Implications for arsenic mobility. *Environ. Sci. Technol.* **2003**, *37* (18), 4182–4189.
(4) Tufano, K. J.; Reyes, C.; Saltikov, C. W.; Fendorf, S. E. reductive processes controlling arsenic retention: Revealing the relative importance of iron and arsenic reduction. *Environ. Sci. Technol.* **2008**, *42* (22), 8283–8289.
(5) Arai, Y.; Elzinga, E. J.; Sparks, D. L. X-ray absorption spectroscopic investigation of arsenite and arsenate adsorption at the aluminum oxide–water interface. *J. Colloid Interface Sci.* **2001**, *235* (1), 80–88.
(6) Root, R.; Dixit, S.; Campbell, K. M.; Jew, A.; Hering, J. G.; O'day, P. A. Arsenic sequestration by sorption processes in high-iron sediments. *Geochim. Cosmochim. Acta* **2007**, *71* (23), 5782–5803.
(7) Troyer, L. D.; Stone, J. J.; Borch, T. Effect of biogeochemical redox processes on the fate and transport of As and U at an abandoned uranium mine site: an X-ray absorption spectroscopy study. *Envir. Chem.* **2014**, *11* (1), 18–27.
(8) Borch, T.; Roche, N.; Johnson, T. E. Determination of contaminant levels and remediation efficacy in groundwater at a former in situ recovery uranium mine. *J. Environ. Monit.* **2012**, *14* (7), 1814.
(9) Larson, L. N.; Kipp, G. G.; Mott, H. V.; Stone, J. J. Sediment pore-water interactions associated with arsenic and uranium transport from the North Cave Hills mining region, South Dakota, USA. *Appl. Geochem.* **2012**, *27* (4), 879–891.
(10) Rutsch, M.; Geipel, G.; Brendler, V.; Bernhard, G.; Nitsche, H. Interaction of uranium(VI) with arsenate(V) in aqueous solution studied time-resolved laser-induced fluorescence spectroscopy (TRLFS). *Radiochim. Acta* **1999**, *86* (3–4), 135–141.
(11) Gezahegne, W. A.; Hennig, C.; Tsushima, S.; Planer-Friedrich, B.; Scheinost, A. C.; Merkel, B. J.; EXAFS, D. F. T. investigations of

uranyl arsenate complexes in aqueous solution. *Environ. Sci. Technol.* **2012**, *46* (4), 2228−2233.

(12) Tang, Y.; Reeder, R. J. Uranyl and arsenate cosorption on aluminum oxide surface. *Geochim. Cosmochim. Acta* **2009**, *73* (10), 2727−2743.

(13) Nipruk, O. V.; Chernorukov, N. G.; Pykhova, Y. P.; Godovanova, N. S.; Eremina, A. A. State of uranyl phosphates and arsenates in aqueous solutions. *Radiochemistry* **2011**, *53* (5), 483−490.

(14) Singh, A.; Ulrich, K.-U.; Giammar, D. E. Impact of phosphate on U(VI) immobilization in the presence of goethite. *Geochim. Cosmochim. Acta* **2010**, *74* (22), 6324−6343.

(15) Singh, A.; Catalano, J. G.; Ulrich, K.-U.; Giammar, D. E. Molecular-scale structure of uranium(VI) immobilized with goethite and phosphate. *Environ. Sci. Technol.* **2012**, *46* (12), 6594−6603.

(16) Cheng, T.; Barnett, M. O.; Roden, E. E.; Zhuang, J. Effects of phosphate on uranium (VI) adsorption to goethite-coated sand. *Environ. Sci. Technol.* **2004**, *38* (22), 6059−6065.

(17) Sivaswamy, V.; Boyanov, M. I.; Peyton, B. M.; Viamajala, S.; Gerlach, R.; Apel, W. A.; Sani, R. K.; Dohnalkova, A.; Kemner, K. M.; Borch, T. Multiple mechanisms of uranium immobilization by Cellulomonas sp. strain ES6. *Biotechnol. Bioeng.* **2011**, *108* (2), 264−276.

(18) Salome, K. R.; Green, S. J.; Beazley, M. J.; Webb, S. M.; Kostka, J. E.; Taillefert, M. The role of anaerobic respiration in the immobilization of uranium through biomineralization of phosphate minerals. *Geochim. Cosmochim. Acta* **2013**, *106* (C), 344−363.

(19) Beazley, M. J.; Martinez, R. J.; Sobecky, P. A.; Webb, S. M.; Taillefert, M. Nonreductive biomineralization of uranium(VI) phosphate via microbial phosphatase activity in anaerobic conditions. *Geomicrobiol. J.* **2009**, *26* (7), 431−441.

(20) Beazley, M. J.; Martinez, R. J.; Sobecky, P. A.; Webb, S. M.; Taillefert, M. Uranium biomineralization as a result of bacterial phosphatase activity: Insights from bacterial isolates from a contaminated subsurface. *Environ. Sci. Technol.* **2007**, *41* (16), 5701−5707.

(21) Simon, F. G.; Biermann, V.; Peplinski, B. Uranium removal from groundwater using hydroxyapatite. *Appl. Geochem.* **2008**, *23* (8), 2137−2145.

(22) Fuller, C. C.; Bargar, J. R.; Davis, J. A.; Piana, M. J. Mechanisms of uranium interactions with hydroxyapatite: Implications for groundwater remediation. *Environ. Sci. Technol.* **2002**, *36* (2), 158−165.

(23) Boyanov, M. I.; Fletcher, K. E.; Kwon, M. J.; Rui, X.; O'Loughlin, E. J.; Löffler, F. E.; Kemner, K. M. Solution and microbial controls on the formation of reduced U(IV) species. *Environ. Sci. Technol.* **2011**, *36* (2), 158−165.

(24) Ray, A. E.; Bargar, J. R.; Sivaswamy, V.; Dohnalkova, A. C.; Fujita, Y.; Peyton, B. M.; Magnuson, T. S. Evidence for multiple modes of uranium immobilization by an anaerobic bacterium. *Geochim. Cosmochim. Acta* **2011**, *75* (10), 2684−2695.

(25) Bernier-Latmani, R.; Veeramani, H.; Vecchia, E. D.; Junier, P.; Lezama-Pacheco, J. S.; Suvorova, E. I.; Sharp, J. O.; Wigginton, N. S.; Bargar, J. R. Non-uraninite products of microbial U(VI) reduction. *Environ. Sci. Technol.* **2010**, *44* (24), 9456−9462.

(26) Rui, X.; Kwon, M. J.; O'Loughlin, E. J.; Dunham-Cheatham, S.; Fein, J. B.; Bunker, B.; Kemner, K. M.; Boyanov, M. I. Bioreduction of hydrogen uranyl phosphate: mechanisms and U(IV) products. *Environ. Sci. Technol.* **2013**, *47* (11), 5668−5678.

(27) Khijniak, T. V.; Slobodkin, A. I.; Coker, V.; Renshaw, J. C.; Livens, F. R.; Bonch-Osmolovskaya, E. A.; Birkeland, N. K.; Medvedeva-Lyalikova, N. N.; Lloyd, J. R. Reduction of uranium(VI) phosphate during growth of the thermophilic bacterium *Thermoterrabacterium ferrireducens*. *Appl. Environ. Microbiol.* **2005**, *71* (10), 6423−6426.

(28) Tang, Y.; Reeder, R. J. Enhanced uranium sorption on aluminum oxide pretreated with arsenate. Part I: Batch uptake behavior. *Environ. Sci. Technol.* **2009**, *43* (12), 4446−4451.

(29) Tang, Y.; Mcdonald, J.; Reeder, R. J. Enhanced uranium sorption on aluminum oxide pretreated with arsenate. Part II:

Spectroscopic studies. *Environ. Sci. Technol.* **2009**, *43* (12), 4452−4458.

(30) Wu, W.-M.; Carley, J.; Gentry, T.; Ginder-Vogel, M.; Fienen, M.; Mehlhorn, T. Pilot-scale in situ bioremedation of uranium in a highly contaminated aquifer. 2. Reduction of U(VI) and geochemical control of U(VI) bioavailability. *Environ. Sci. Technol.* **2006**, *40* (12), 3986−3995.

(31) Wu, W.-M.; Carley, J.; Luo, J.; Ginder-Vogel, M.; Cardenas, E.; Leigh, M.; Hwang, C.; Kelly, S.; Ruan, C.; Wu, L. In situ bioreduction of uranium(VI) to submicromolar levels and reoxidation by dissolved oxygen. *Environ. Sci. Technol.* **2007**, *41* (16), 5716−5723 DOI: 10.1021/es062657b.

(32) Lovley, D. R.; Gorby, Y. A. Enzymatic uranium precipitation. *Environ. Sci. Technol.* **1992**, *26* (11), 205−207.

(33) Lovley, D. R.; Phillips, E. J. P.; Gorby, Y. A.; Landa, E. R. Microbial reduction of uranium. *Nature* **1991**, *350*, 413−416.

(34) Wall, J. D.; Krumholz, L. R. Uranium reduction. *Annu. Rev. Microbiol.* **2006**, *60*, 149−166.

(35) Postma, D.; Jakobsen, R. Redox zonation: Equilibrium constraints on the $Fe(III)/SO_4^-$ reduction interface. *Geochim. Cosmochim. Acta* **1996**, *60* (17), 3169−3175.

(36) Burkhardt, E.-M.; Akob, D. M.; Bischoff, S.; Sitte, J.; Kostka, J. E.; Banerjee, D.; Scheinost, A. C.; Küsel, K. Impact of biostimulated redox processes on metal dynamics in an iron-rich creek soil of a former uranium mining area. *Environ. Sci. Technol.* **2010**, *44* (1), 177−183.

(37) Anderson, R. T.; Vrionis, H. A.; Ortiz-Bernad, I.; Resch, C. T.; Long, P. E.; Dayvault, R.; Karp, K.; Marutzky, S.; Metzler, D. R.; Peacock, A.; et al. Stimulating the in situ activity of Geobacter species to remove uranium from the groundwater of a uranium-contaminated aquifer. *Appl. Environ. Microbiol.* **2003**, *69* (10), 5884−5891.

(38) Berner, R. A. Thermodynamic stability of sedimentary iron sulfides. *Am. J. Sci.* **1967**, *265* (9), 773−785.

(39) Rickard, D.; Luther, G. W. Chemistry of iron sulfides. *Science* **2007**, *107* (2), 514−562.

(40) Rickard, D. Kinetics of FeS precipitation: Part 1. Competing reaction mechanisms. *Geochim. Cosmochim. Acta* **1995**, *59* (21), 4367−4379.

(41) Wilkin, R. T.; Barnes, H. L. Pyrite formation by reactions of iron monosulfides with dissolved inorganic and organic sulfur species. *Geochim. Cosmochim. Acta* **1996**, *60* (21), 4167−4179.

(42) Hua, B.; Deng, B. Reductive immobilization of uranium(VI) by amorphous iron sulfide. *Environ. Sci. Technol.* **2008**, *42* (23), 8703−8708.

(43) Hyun, S. P.; Davis, J. A.; Sun, K.; Hayes, K. F. Uranium(VI) reduction by iron(II) monosulfide mackinawite. *Environ. Sci. Technol.* **2012**, *46* (6), 3369−3376.

(44) Veeramani, H.; Scheinost, A. C.; Monsegue, N.; Qafoku, N. P.; Kukkadapu, R.; Newville, M.; Lanzirotti, A.; Pruden, A.; Murayama, M.; Hochella, M. F., Jr. Abiotic reductive immobilization of U (VI) by biogenic mackinawite. *Environ. Sci. Technol.* **2013**, *47* (5), 2361−2369.

(45) Bargar, J. R.; Williams, K. H.; Campbell, K. M.; Long, P. E.; Stubbs, J. E.; Suvorova, E. I.; Lezama-Pacheco, J. S.; Alessi, D. S.; Stylo, M.; Webb, S. M. Uranium redox transition pathways in acetate-amended sediments. *Proc. Natl. Acad. Sci. U.S.A.* **2013**, *110* (12), 4506−4511.

(46) Abdelouas, A.; Lutze, W.; Nuttall, H. Oxidative dissolution of uraninite precipitated on Navajo sandstone. *J. Contam. Hydrol.* **1999**, *36* (3–4), 353−375.

(47) Bi, Y.; Hayes, K. F. Nano-FeS inhibits UO_2 reoxidation under varied oxic conditions. *Environ. Sci. Technol.* **2014**, *48* (1), 632−640.

(48) Gallegos, T. J.; Han, Y.-S.; Hayes, K. F. Model predictions of realgar precipitation by reaction of As(III) with synthetic mackinawite under anoxic conditions. *Environ. Sci. Technol.* **2008**, *42* (24), 9338−9343.

(49) Gallegos, T. J.; Hyun, S. P.; Hayes, K. F. Spectroscopic investigation of the uptake of arsenite from solution by synthetic mackinawite. *Environ. Sci. Technol.* **2007**, *41* (22), 7781−7786.

(50) Kocar, B. D.; Borch, T.; Fendorf, S. Arsenic repartitioning during biogenic sulfidization and transformation of ferrihydrite. *Geochim. Cosmochim. Acta* **2010**, *74* (3), 980−994.

(51) Burton, E. D.; Johnston, S. G.; Bush, R. T. Microbial sulfidogenesis in ferrihydrite-rich environments: Effects on iron mineralogy and arsenic mobility. *Geochim. Cosmochim. Acta* **2011**, *75* (11), 3072−3087.

(52) Butler, E. C.; Hayes, K. F. Effects of solution composition and pH on the reductive dechlorination of hexachloroethane by iron sulfide. *Environ. Sci. Technol.* **1998**, *32* (9), 1276−1284.

(53) Amstaetter, K.; Borch, T.; Larese-Casanova, P.; Kappler, A. Redox transformation of arsenic by Fe (II)-activated goethite (α-FeOOH). *Environ. Sci. Technol.* **2010**, *44* (1), 102−108.

(54) Stookey, L. Ferrozine—a new spectrophotometric reagent for iron. *Anal. Chem.* **1970**, *42* (7), 779−781.

(55) Webb, S. M. SIXPACK: a graphical user interface for XAS analysis using IFEFFIT. *Phys. Scr.* **2005**, *115*, 1011−1014.

(56) Ravel, B.; Newville, M. ATHENA, ARTEMIS, HEPHAESTUS: data analysis for X-ray absorption spectroscopy using IFEFFIT. *J. Synchrotron Radiat.* **2005**, *12* (4), 537−541.

(57) Newville, M.; Carroll, S. A.; O'day, P. A.; Waychunas, G. A.; Ebert, M. A web-based library of XAFS data on model compounds. *J. Synchrotron Radiat.* **1999**, *6* (3), 276−277.

(58) Bostick, B. C.; Chen, C.; Fendorf, S. E. Arsenite retention mechanisms within estuarine sediments of Pescadero, CA. *Environ. Sci. Technol.* **2004**, *38* (12), 3299−3304.

(59) Gu, B.; Wu, W.-M.; Ginder-Vogel, M.; Yan, H.; Fields, M.; Zhou, J.; Fendorf, S. E.; Criddle, C. S.; Jardine, P. M. Bioreduction of uranium in a contaminated soil column. *Environ. Sci. Technol.* **2005**, *39* (13), 4841−4847.

(60) Borch, T.; Masue-Slowey, Y.; Kukkadapu, R. K.; Fendorf, S. E. Phosphate imposed limitations on biological reduction and alteration of ferrihydrite. *Environ. Sci. Technol.* **2007**, *41* (1), 166−172.

(61) Ressler, T. WinXAS: A new software package not only for the analysis of energy-dispersive XAS data. *J. Phys. IV Fr.* **1997**, *7* (C2), 269−270.

(62) Newville, M. IFEFFIT: interactive XAFS analysis and FEFF fitting. *J. Synchrotron Radiat.* **2001**, *8* (2), 322−324.

(63) Zabinsky, S. I.; Rehr, J. J.; Ankudinov, A.; Albers, R. C.; Eller, M. J. FEFF code for ab initio calculations of XAFS. *Phys. Rev. B* **1995**, *52* (4), 2995−3009.

(64) Appelo, C.; Parkhurst, D. L. Description of input and examples for PHREEQC version 3—a computer program for speciation, batch-reaction, one-dimensional transport, and inverse geochemical calculations; U.S. Geological Survey: Reston, VA, 2013; Vol. *A43*.

(65) Hyun, S. P.; Davis, J. A.; Hayes, K. F. Abiotic U(VI) reduction by aqueous sulfide. *Appl. Geochem.* **2014**, *50*, 7−15.

(66) Moyes, L. N.; Parkman, R. H.; Charnock, J. M.; Vaughan, D. J.; Livens, F. R.; Hughes, C. R.; Braithwaite, A. Uranium uptake from aqueous solution by interaction with goethite, lepidocrocite, muscovite, and mackinawite: An X-ray absorption spectroscopy study. *Environ. Sci. Technol.* **2000**, *34* (6), 1062−1068.

(67) Livens, F. R.; Jones, M. J.; Hynes, A. J.; Charnock, J. M.; Mosselmans, J. F. W.; Hennig, C.; Steele, H.; Collison, D.; Vaughan, D. J.; Pattrick, R. A. D.; et al. X-ray absorption spectroscopy studies of reactions of technetium, uranium and neptunium with mackinawite. *J. Environ. Radioactiv* **2004**, *74* (1−3), 211−219.

(68) Geipel, G.; Bernhard, G.; Brendler, V. Complex Formation of Uranium(IV) with Phosphate and Arsenate. In *Uranium in the aquatic environment: Proceedings of the international conference [on] uranium mining and hydrogeology III and the international mine water association symposium*; Freiberg, Germany, 15−21 Sep, 2002; Merkel, B., Planer-Friedrich, B., Wolkersdorfer, C., Eds.; Springer: New York, 2002; p 369.

(69) Burns, P. C. U^{6+} minerals and inorganic compounds: insights into an expanded structural hierarchy of crystal structures. *Can. Mineral.* **2005**, *43* (6), 1839−1894.

(70) Burns, P.; Finch, R., Eds. *Uranium: mineralogy, geochemistry, and the environment*; Mineralogical Society of America: Washington, D.C., 1999.

(71) Wolthers, M.; Charlet, L.; van Der Linde, P. R.; Rickard, D.; van Der Weijden, C. H. Surface chemistry of disordered mackinawite (FeS). *Geochim. Cosmochim. Acta* **2005**, *69* (14), 3469−3481.

(72) Jeong, H. Y.; Lee, J. H.; Hayes, K. Characterization of synthetic nanocrystalline mackinawite: Crystal structure, particle size, and specific surface area. *Geochim. Cosmochim. Acta* **2008**, *72* (2), 493−505.

(73) Kirk, M. F.; Roden, E. E.; Crossey, L. J.; Brealey, A. J.; Spilde, M. N. Experimental analysis of arsenic precipitation during microbial sulfate and iron reduction in model aquifer sediment reactors. *Geochim. Cosmochim. Acta* **2010**, *74* (9), 2538−2555.

(74) Wolthers, M.; Charlet, L.; van Der Weijden, C. H.; van Der Linde, P. R.; Rickard, D. Arsenic mobility in the ambient sulfidic environment: Sorption of arsenic (V) and arsenic (III) onto disordered mackinawite. *Geochim. Cosmochim. Acta* **2005**, *69* (14), 3483−3492.

(75) Widler, A. M.; Seward, T. M. The adsorption of gold (I) hydrosulphide complexes by iron sulphide surfaces. *Geochim. Cosmochim. Acta* **2002**, *66* (3), 383−402.

(76) Bebie, J.; Schoonen, M. A.; Fuhrmann, M.; Strongin, D. R. Surface charge development on transition metal sulfides: an electro-kinetic study. *Geochim. Cosmochim. Acta* **1998**, *62* (4), 633−642.

(77) Bostick, B. C. Arsenite sorption on troilite (FeS) and pyrite (FeS$_2$). *Geochim. Cosmochim. Acta* **2003**, *67* (5), 909−921.

(78) Suess, E.; Planer-Friedrich, B. Thioarsenate formation upon dissolution of orpiment and arsenopyrite. *Chemosphere* **2012**, *89* (11), 1390−1398.

(79) Suess, E.; Wallschläger, D.; Planer-Friedrich, B. Stabilization of thioarsenates in iron-rich waters. *Chemosphere* **2011**, *83* (11), 1524−1531.

(80) Couture, R. M.; Rose, J.; Kumar, N.; Mitchell, K.; Wallschläger, D.; Van Cappellen, P. Sorption of arsenite, arsenate, and thioarsenates to iron oxides and iron sulfides: A kinetic and spectroscopic investigation. *Environ. Sci. Technol.* **2013**, *47* (11), 5652−5659.

(81) Planer-Friedrich, B.; Suess, E.; Scheinost, A. C.; Wallschläger, D. Arsenic speciation in sulfidic waters: Reconciling contradictory spectroscopic and chromatographic evidence. *Anal. Chem.* **2010**, *82* (24), 10228−10235.

(82) Petrick, J. S.; Ayala-Fierro, F.; Cullen, W. R.; Carter, D. E.; Vasken Aposhian, H. Monomethylarsonous acid (MMA^{III}) is more toxic than arsenite in chang human hepatocytes. *Toxicol. Appl. Pharmacol.* **2000**, *163* (2), 203−207.

(83) Tokunaga, T. K.; Kim, Y.; Wan, J.; Yang, L. Aqueous uranium(VI) concentrations controlled by calcium uranyl vanadate precipitates. *Environ. Sci. Technol.* **2012**, *46* (14), 7471−7477.

(84) Tokunaga, T. K.; Kim, Y.; Wan, J. Potential remediation approach for uranium-contaminated groundwaters through potassium uranyl vanadate precipitation. *Environ. Sci. Technol.* **2009**, *43* (14), 5467−5471.